12th Symposium on Overset Composite Grids and Solution Technology

Georgia Institute of Technology
Oct 9, 2014

Development of a High-Order Strand Solver for Helios

TECHNOLOGY DRIVEN. WARFIGHTER FOCUSED.

Andrew Wissink, *U.S. Army* Aviation Development Directorate - AFDD
Jayanarayanan Sitaraman, *Parallel Geometric Alg LLC*
Aaron Katz, *Utah State University*

Presented by:

Dr. Jayanarayanan Sitaraman

Parallel Geometric Algorithms, LLC

Outline

- **Background & Motivation**
- **High-order Solver formulation**
- **Preliminary Results**
- **Summary and Conclusions**

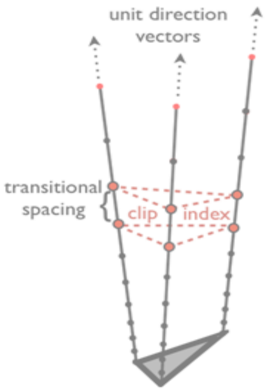

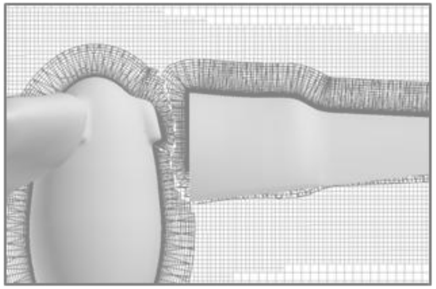

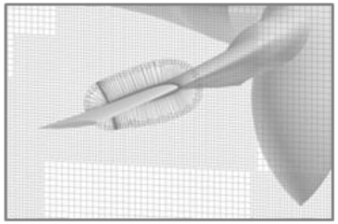

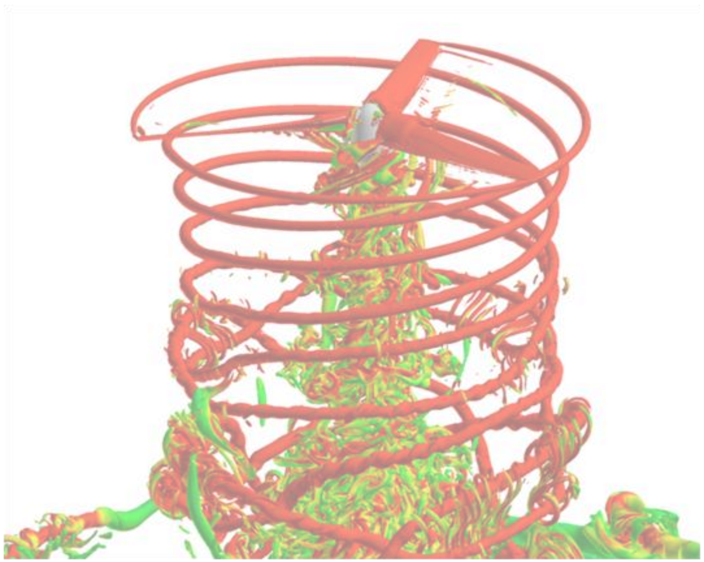

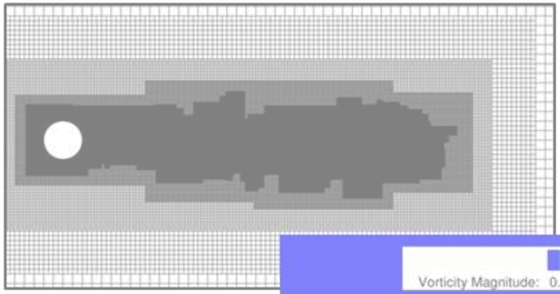

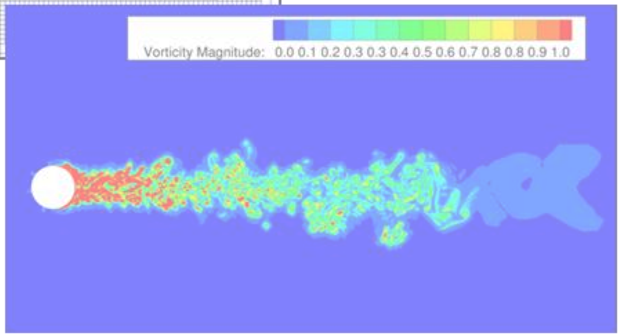

Background

UH-60 “Blackhawk”

CH-47 “Chinook”

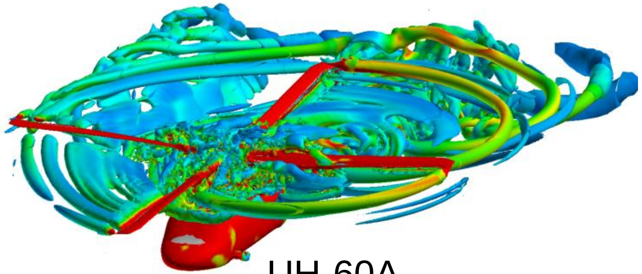

UH-60A

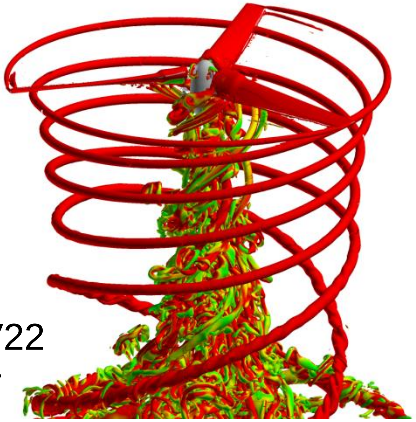

Model V22 Rotor

- **Complexities in high fidelity rotary-wing aeromechanics prediction**
  - Complex geometries
  - High-Re wall-bounded viscous flow
  - Wake resolution
  - Strong aero-structure coupling, particularly blade twist from pitching moment

Issue #1: Automation

- Rotorcraft CFD steps

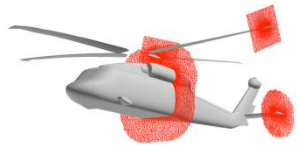

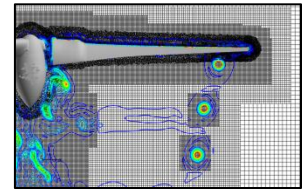

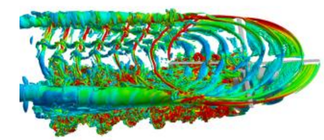

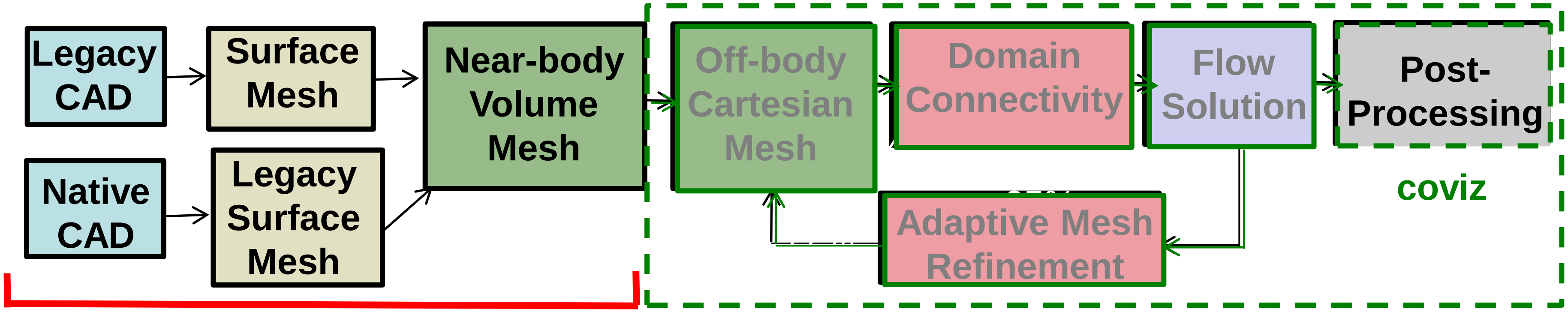

NOT AUTOMATED

Mostly Automated in CREATE™-AV HELIOS code

How do we enable skilled rotorcraft engineers to use high-fidelity CFD tools without forcing them to become grid generation experts?

JMR Concept

Issue #2: Accuracy

- **Lower order near-body solver limits ability to resolve tip rollup**

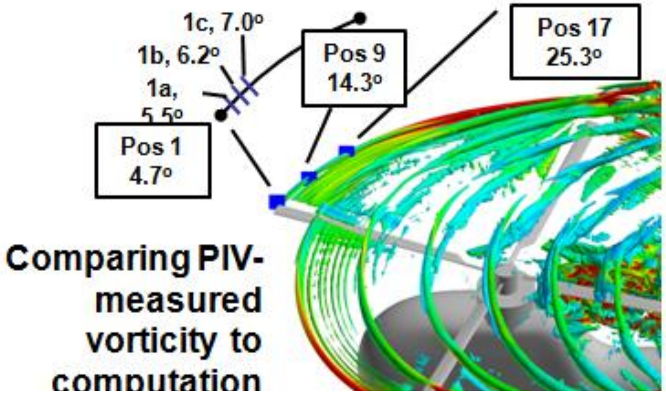

HART-II

Tip vortex expansion

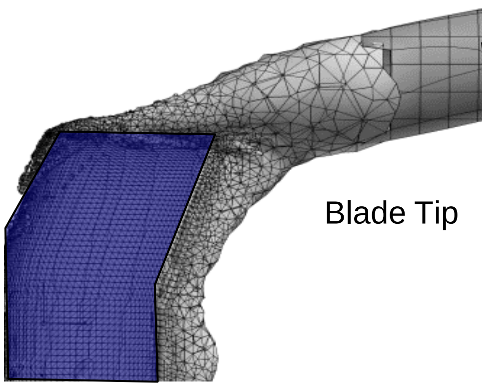

Blade Tip

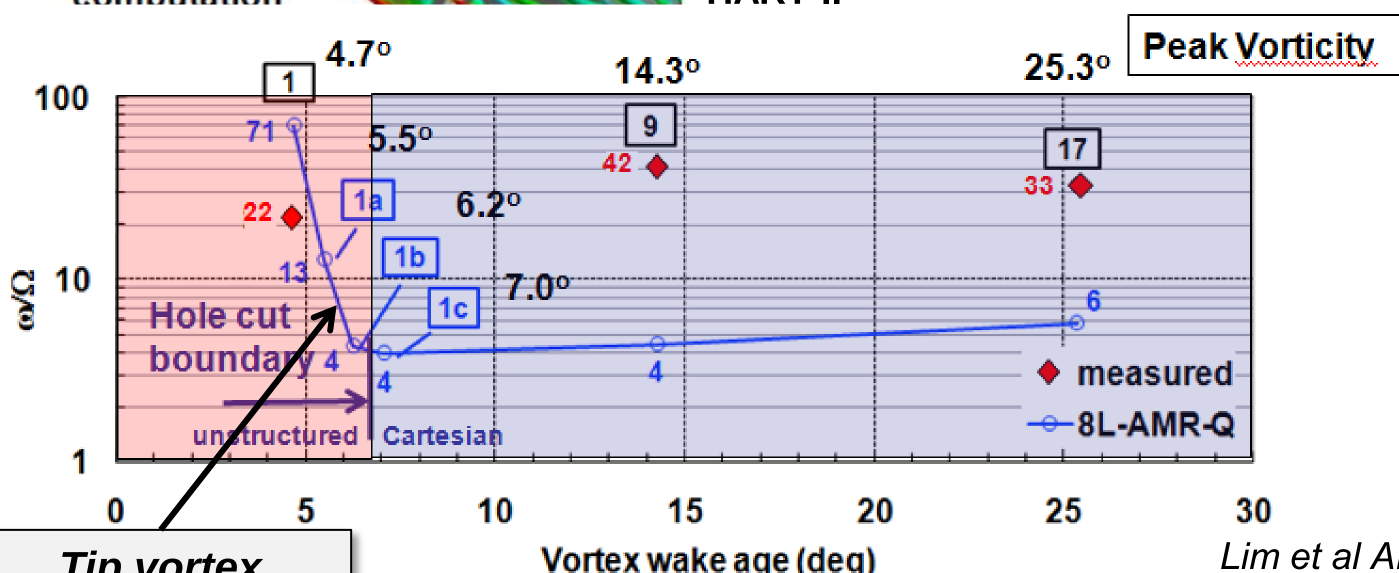

Lim et al AHS Forum'2012

Tip vortex dissipation

Issue #3: Speed

- **Near-body solver is the most expensive portion of the simulation**

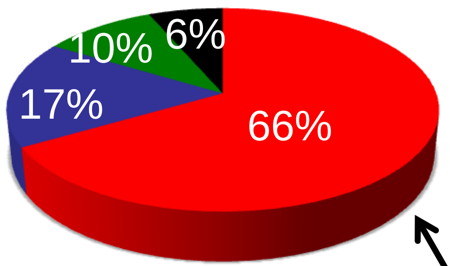

Model V22 Hover - **128 procs**

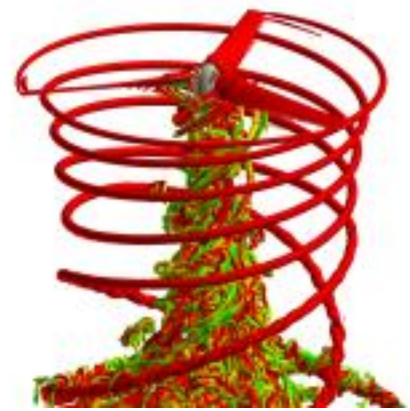

Two-thirds total cost

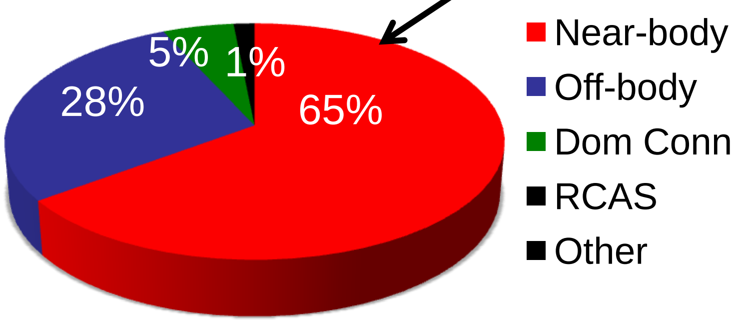

UH60 Fwd Flight – **512 procs**

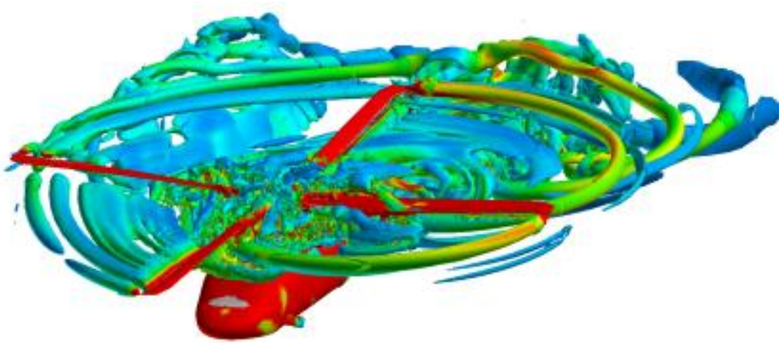

Strand Technology Addresses these Issues

- **Automation**
  - Near-body strands grown directly from surface tessellation
  - Cartesian off-body resolution adjusted according by available compute resources
  - ***Strand-Cartesian volume mesh generated automatically at runtime***

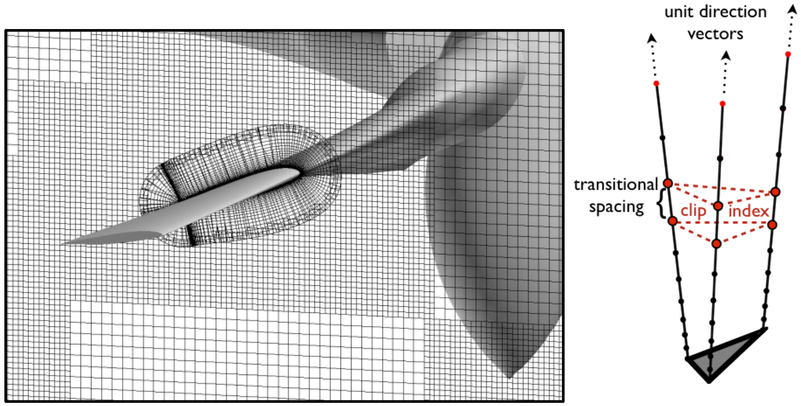

- **Accuracy & Efficiency**
  - High-order solver formulation that takes advantage of strand data structure
  - Fast and scalable domain connectivity
  - Structured data ensures fast numerics
  - ***4^{th} order solutions at only 1.5X cost of 2^{nd} order solutions***

Flow over cylinder

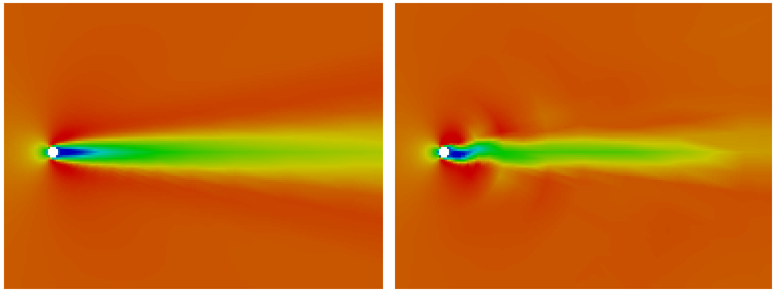

2^{nd}-O 4^{th}-O

Outline

- Background & Motivation
- **High-order Solver formulation**
- Preliminary Results
- Summary and Conclusions

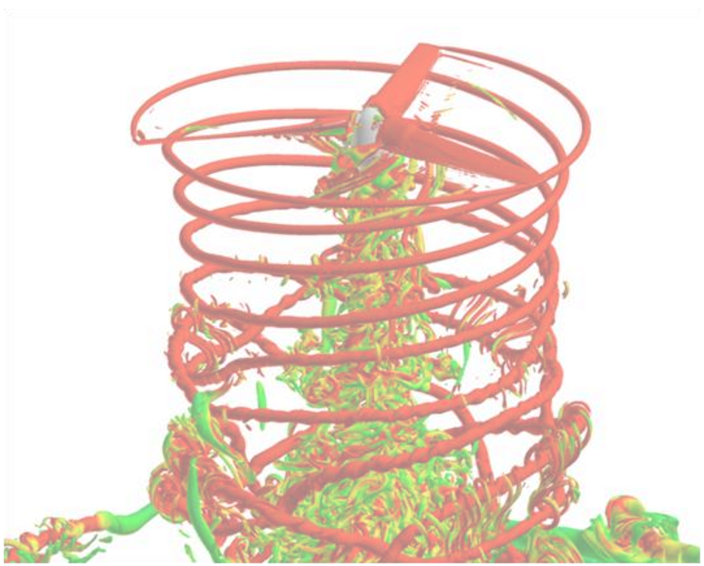

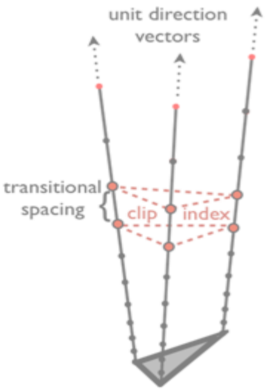

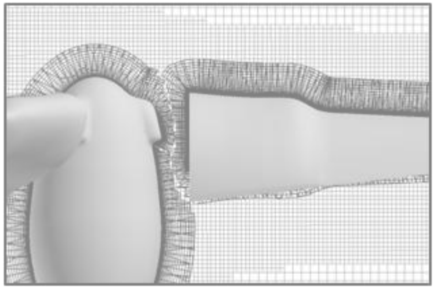

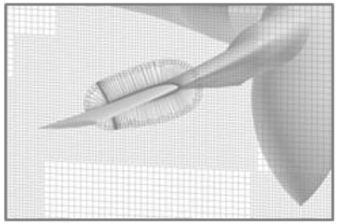

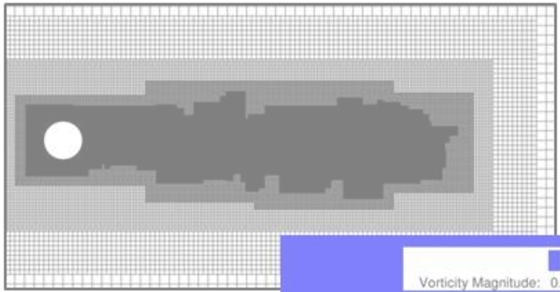

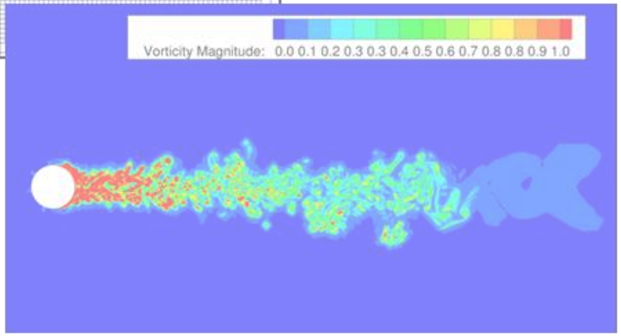

High Order Approach

- **Strand <u>normal</u> direction:**
  High Order Finite Differences
  – Summation by parts with variable coefficients
  – Reduces to finite difference at interior
  – Satisfies stability and accuracy constraints

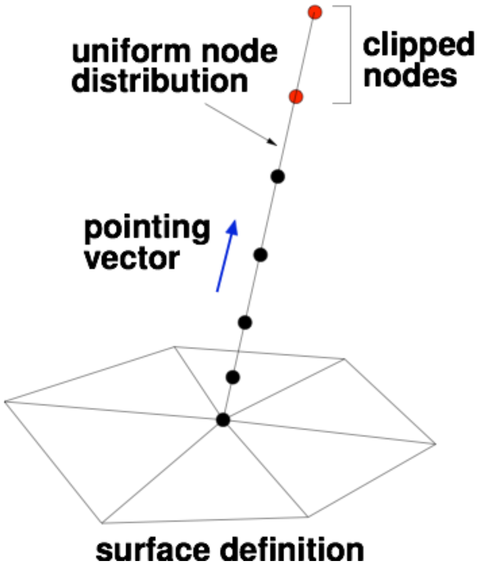

- **Unstructured <u>streamwise</u> direction:**
  High Order Flux corrections
  – Achieves high order through truncation error cancellation of finite volume scheme
  – Layers coupled via source term containing derivatives in strand direction

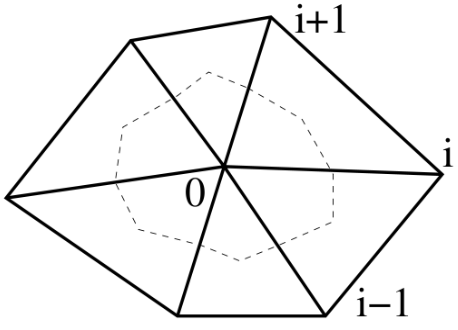

Solver

RANS-SA equations

$$\frac{\partial Q}{\partial t} + \frac{\partial F_j}{\partial x_j} - \frac{\partial F_j^v}{\partial x_j} = S$$

$$Q = \begin{pmatrix} \rho \\ \rho u_i \\ \rho e \\ \rho \tilde{\nu} \end{pmatrix}, \quad F_j = \begin{pmatrix} \rho u_j \\ \rho u_i u_j + p\delta_{ij} \\ \rho h u_j \\ \rho \tilde{\nu} u_j \end{pmatrix}, \quad F_j^v = \begin{pmatrix} 0 \\ \sigma_{ij} \\ \sigma_{ij} u_i - q_j \\ \frac{\eta}{\sigma} \frac{\partial \tilde{\nu}}{\partial x_j} \end{pmatrix}, \quad S = \begin{pmatrix} 0 \\ 0 \\ 0 \\ \mathcal{P} - \mathcal{D} + C_{b2} \rho \frac{\partial \tilde{\nu}}{\partial x_k} \frac{\partial \tilde{\nu}}{\partial x_k} \end{pmatrix}$$

$$\mathcal{P} = \begin{cases} \rho C_{b1} (1 - f_{t2}) \tilde{S} \tilde{\nu}, & \tilde{\nu} \geq 0 \\ \rho C_{b1} (1 - C_{t3}) \Omega \tilde{\nu} & \tilde{\nu} < 0 \end{cases} \qquad \mathcal{D} = \begin{cases} \rho \left(C_{\omega 1} f_\omega - \frac{C_{b1}}{\kappa^2} f_{t2} \right) \left(\frac{\tilde{\nu}}{d} \right)^2, & \tilde{\nu} \geq 0 \\ -\rho C_{\omega 1} \left(\frac{\tilde{\nu}}{d} \right)^2 & \tilde{\nu} < 0 \end{cases}$$

- **Spalart Allmaras turbulence model treatment**
  - Allows negative turbulence working variable (Allmaras 2012)
  - Fully-coupled high-order treatment

Strand Mapping

- **Map from physical to computational space**
  - Equally-spaced sub-triangles in ***r-s*** (streamwise) plane in computational space
    - Cubic or quadratic sub-triangles
  - Stretched node distribution in **η** (normal) direction mapped to equal-spaced distribution in computational space
  - Surface triangles treated as cubic or quadrilateral elements

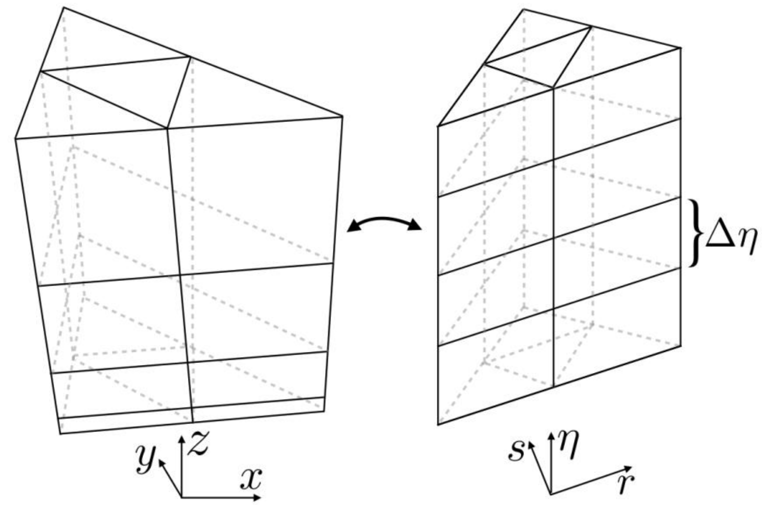

Physical space

Computational space

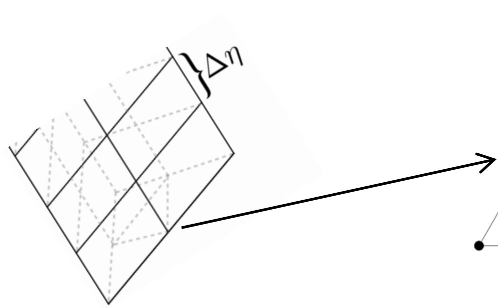

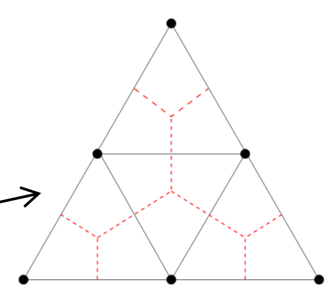

Cubic

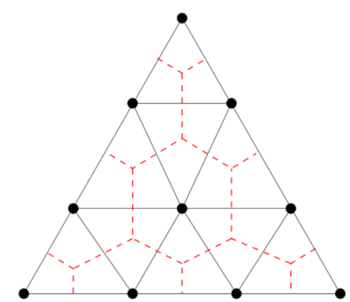

Quadratic

Flux Correction Scheme

- **Finite Volume flux balance**

$$\mathcal{F}^h_{0i} = \frac{1}{2}\left(\mathcal{F}^L_{0i} + \mathcal{F}^R_{0i}\right) - \frac{1}{2}\left|\mathcal{A}(Q^R, Q^L)\right|\left(Q^R - Q^L\right)$$

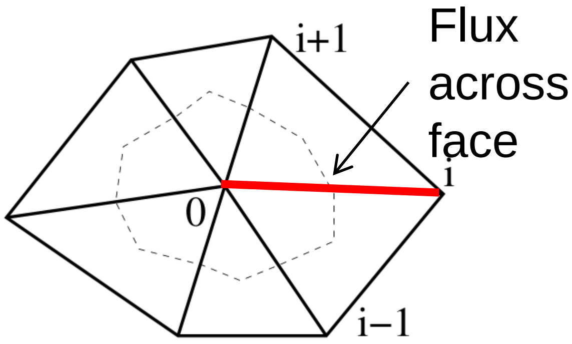

- **Compute left/right fluxes such that truncation error of each cancels when added together**

$$\mathcal{F}^L_{0i} = \mathcal{F}^h_0 + \frac{1}{2}\Delta\boldsymbol{r}^T_{0i}\nabla^h\mathcal{F}^h_0$$

$$\mathcal{F}^R_{0i} = \mathcal{F}^h_i - \frac{1}{2}\Delta\boldsymbol{r}^T_{0i}\nabla^h\mathcal{F}^h_i$$

- **Advantages:**
  - Able to leverage finite volume techniques (shock capturing, efficient solvers, etc.)
  - no high-order quadrature or least squares reconstruction
  - builds on existing infrastructure

Flux Correction Schemes

Previous Work

Katz and Sankaran
J. Sci. Comput. 2012

Subsonic NACA 0012 (steady, inviscid)

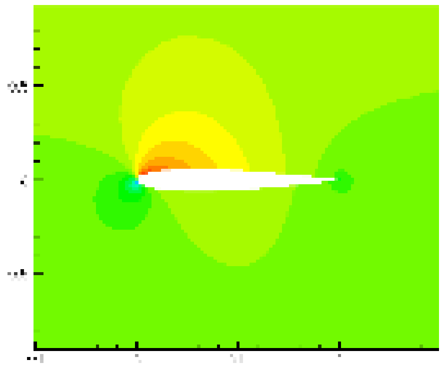

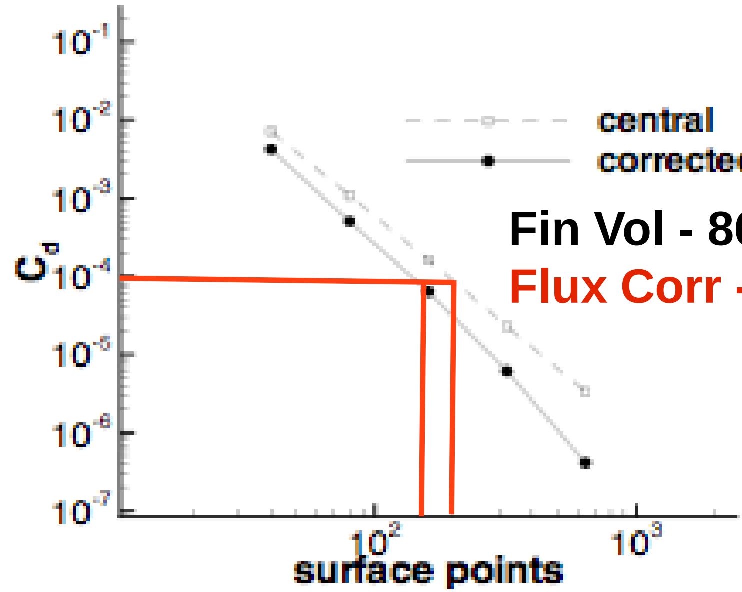

Fin Vol - 8619 nodes
Flux Corr - 4620 nodes

Pincock and Katz,
AIAA-2013-2566

Shedding square (M=0.1, Re=250, ~3000 nodes)

Finite Volume

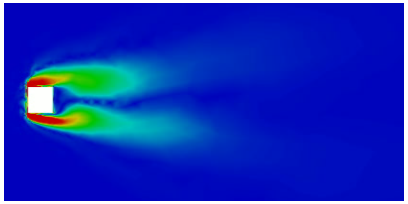

Flux Corr

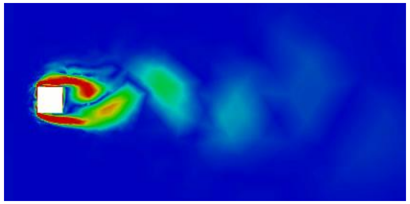

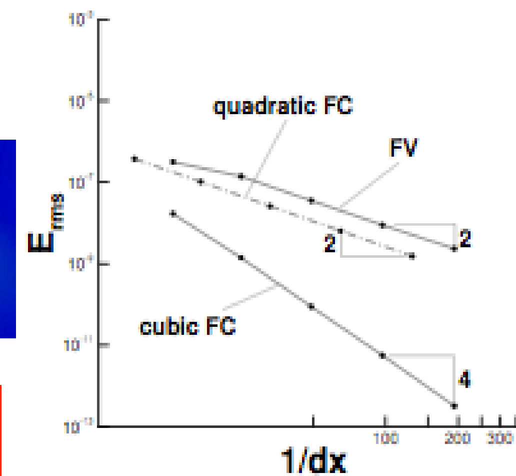

Extend flux corrected schemes to turbulent flows on high aspect ratio strand grids

Strand Direction Coupling

- **Treat strand direction derivatives as source term to preserves flux correction accuracy**

$$\frac{\partial \hat{Q}}{\partial \tau} + \frac{\partial \hat{F}}{\partial r} + \frac{\partial \hat{G}}{\partial s} - \frac{\partial \hat{F}^v}{\partial r} - \frac{\partial \hat{G}^v}{\partial s} = \tilde{S},$$

$$\tilde{S} \equiv \hat{S} - \frac{\partial \hat{Q}}{\partial t} - \frac{\partial \hat{H}}{\partial \eta} + \frac{\partial \hat{H}^v}{\partial \eta}.$$

$$\frac{\partial F}{\partial x} + \frac{\partial G}{\partial y} = S \longrightarrow \frac{\partial F}{\partial x} = \tilde{S}, \quad \tilde{S} \equiv S - D_y G$$

$$D_y G = \partial G / \partial y + O(h^p)$$

Source Treatment

$$\frac{1}{\Delta x_{i,j}} \left[\left(F_{i+\frac{1}{2},j} - F_{i-\frac{1}{2},j} \right) - \tilde{S}^h_{i,j} \right] = \frac{\partial F}{\partial x} + \frac{\partial G}{\partial y} - S - \frac{\Delta x^3_{i+\frac{1}{2}} + \Delta x^3_{i-\frac{1}{2}}}{24 \Delta x_i} \left(F_{3x} - \tilde{S}_{2x} \right) + O(h^p) + O(h^q) + O(h^3).$$

cancels

No Source Treatment

$$\frac{1}{\Delta x_{i,j}} \left[\left(F_{i+\frac{1}{2},j} - F_{i-\frac{1}{2},j} \right) + D_y G_{i,j} - S^h_{i,j} \right] = \frac{\partial F}{\partial x} + \frac{\partial G}{\partial y} - S - \frac{\Delta x^3_{i+\frac{1}{2}} + \Delta x^3_{i-\frac{1}{2}}}{24 \Delta x_i} \left(F_{3x} - S_{2x} \right) + O(h^p) + O(h^q) + O(h^3).$$

does not cancel

Strand Direction

- **High order achieved in strand direction through finite differences**
  - Summation by parts operators
  - Energy stable
  - Fernandez & Zingg, 2012; Mattsson, 2012

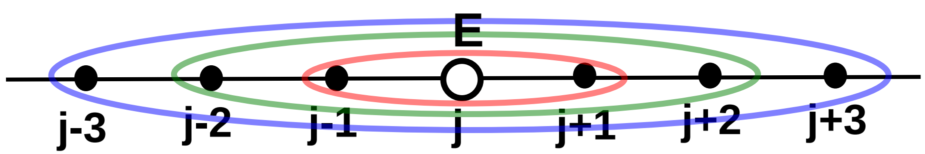

3, 5, 7 point stencil

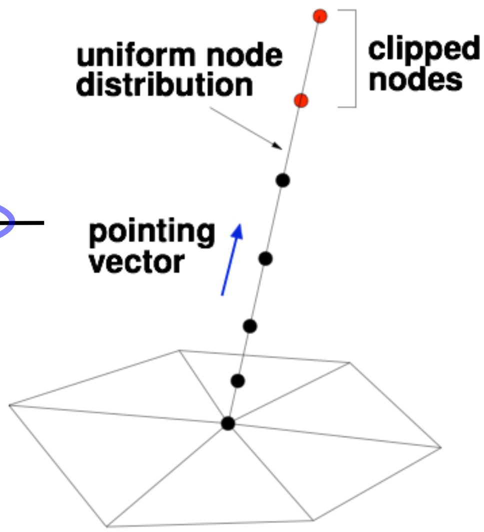

- **Accuracy**
  - 2p interior
  - p boundary
  - p+1 overall
  - Implemented p=1,2,3

Accuracy Verification (cont)

inviscid terms only

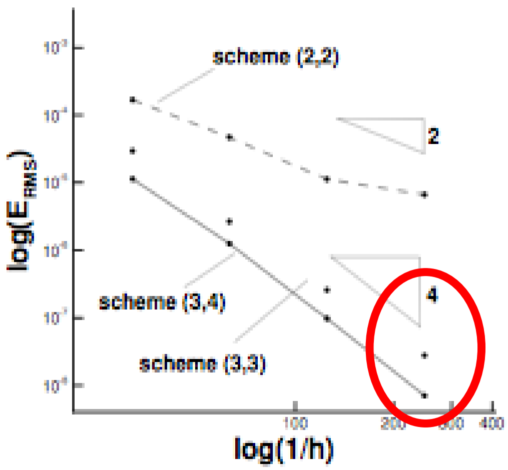

viscous terms only

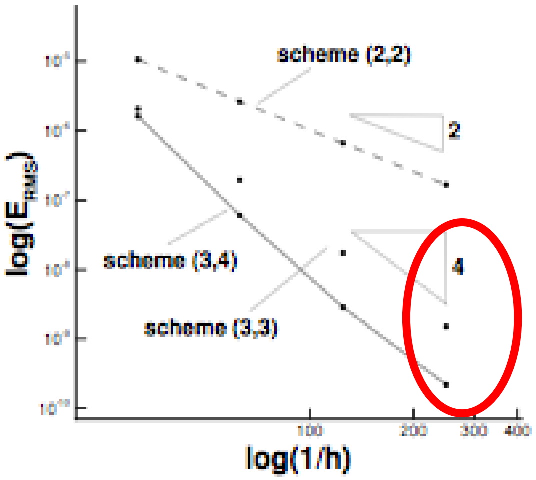

inviscid + viscous

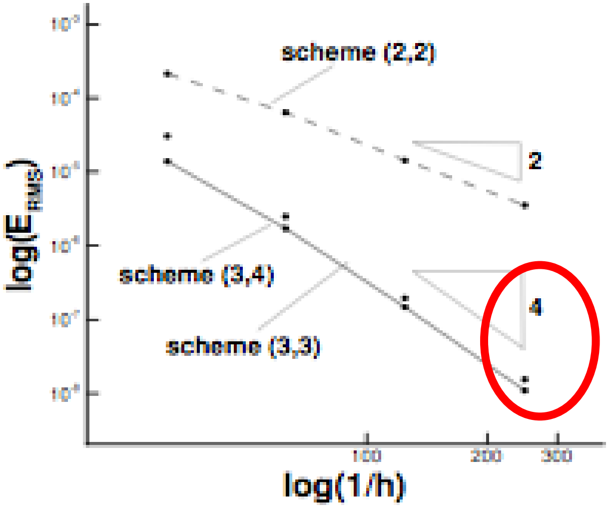

Method of
Manufactured Solns

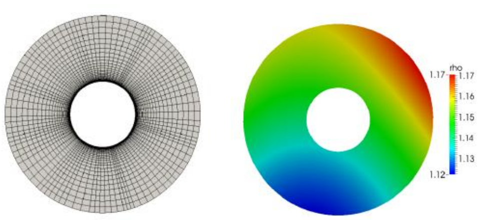

Re=100 Cylinder

3rd-4th Order achieved in tests

Implicit Scheme

- **Semi-implicit Multi-grid scheme**
  - Standard FAS multigrid (Brandt, 1977)
  - LU-SGS (Yoon, Jameson) on strand layers
  - Local RK with implicit smoothing on each unstruct plane (Jameson, Mavriplis)
  - Use of triangles enables 3-element coarsening without agglomoration

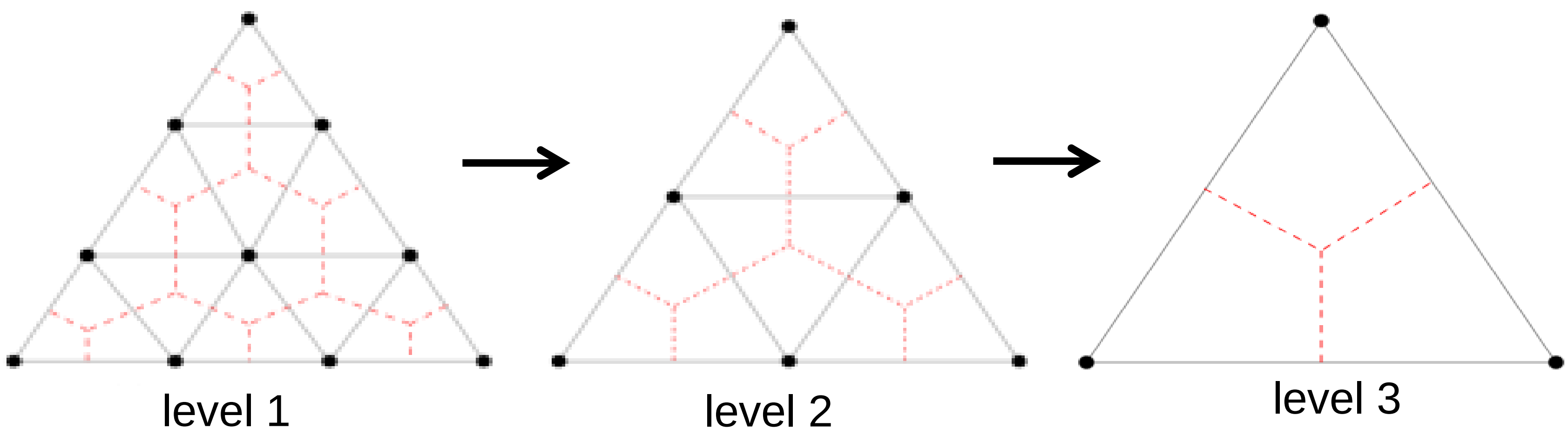

Outline

- Background & Motivation
- High-order Solver formulation
- **Preliminary Results**
- Summary and Conclusions

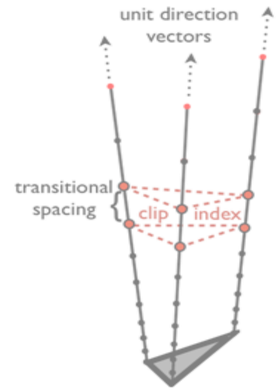

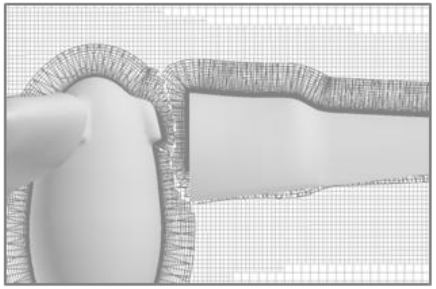

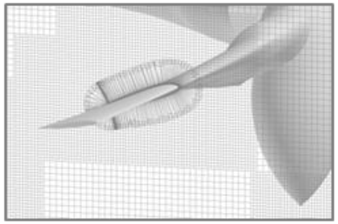

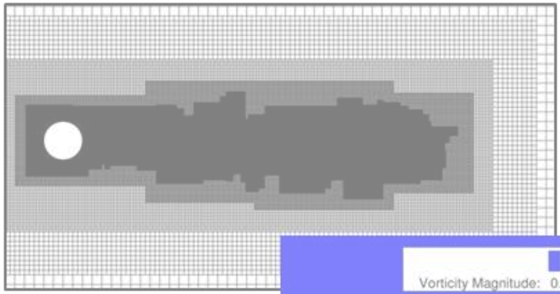

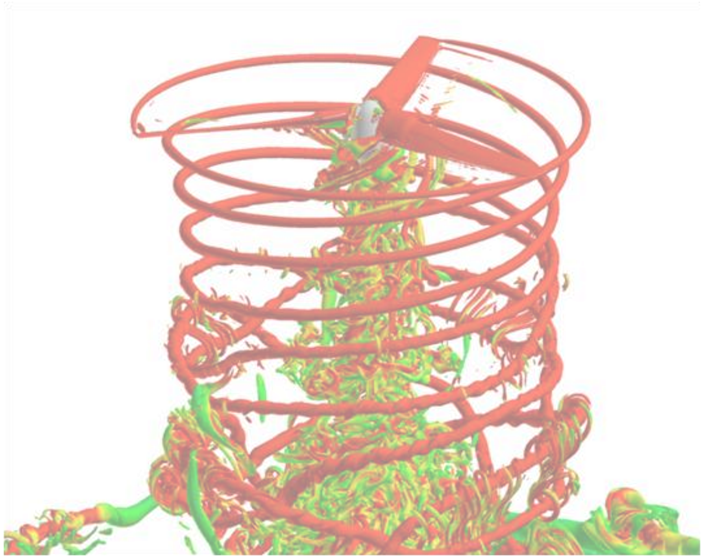

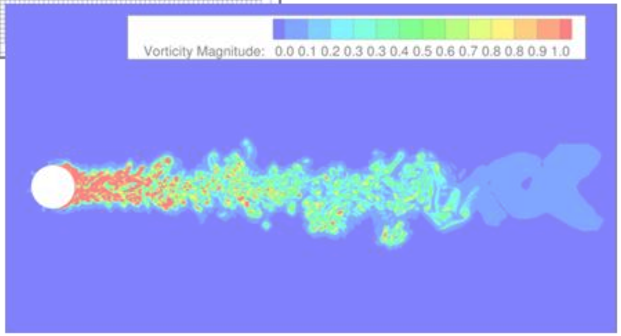

Laminar Flow Validation

- **Flow over circular cylinder**
  - Re=100

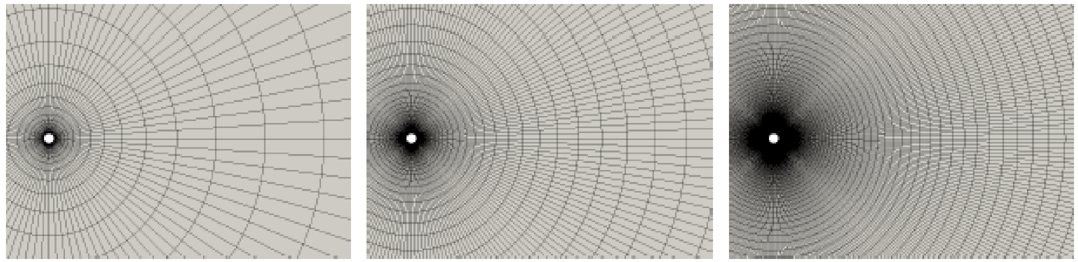

coarse medium fine

Strouhal Number

Mesh	2^{nd} Order	4^{th} Order
Coarse (96x32)	steady	0.141
Medium (192x64)	0.159	0.165
Fine (384x128)	0.177	0.167

*Experiment: St = 0.16-0.17

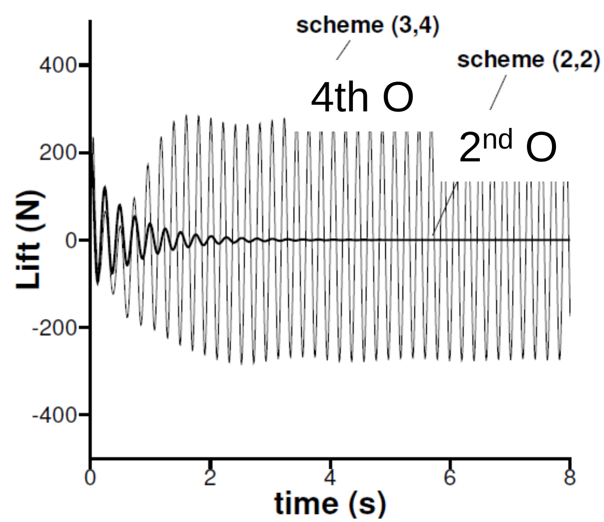

Coarse mesh

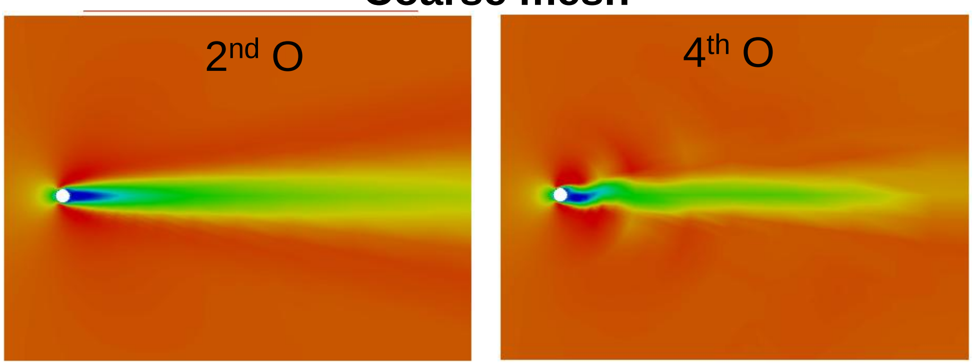

Turbulent Flow Validation

- **Flow over channel bump**
  - M=0.2
  - Re=3 Million
  - 4^{th} order

Turbulent eddy viscosity

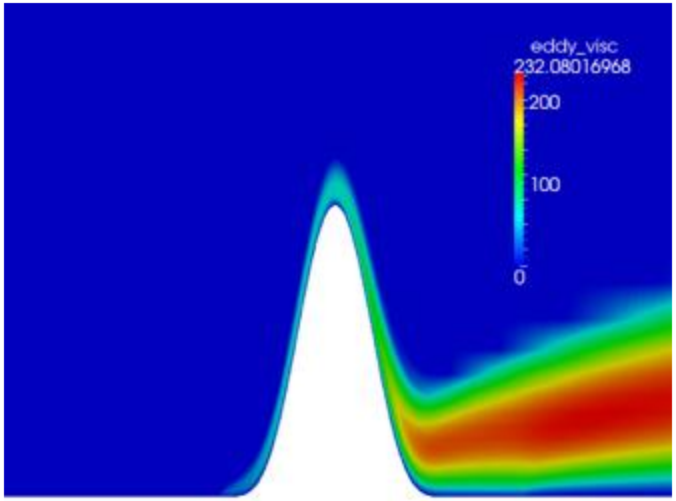

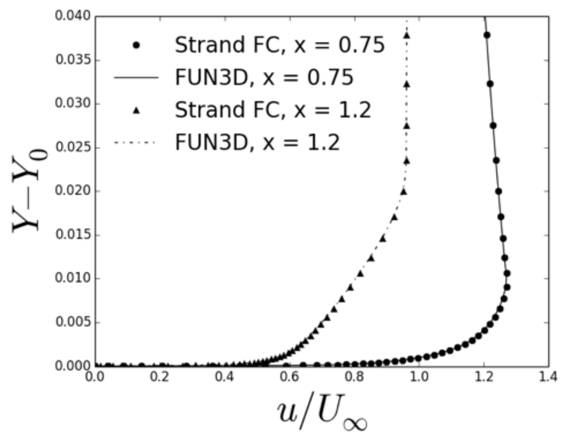

Velocity profile

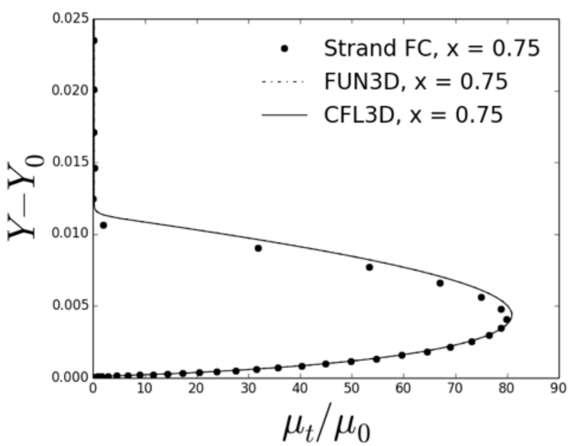

Eddy viscosity profile

Good correlation with NASA's FUN3D, CFL3D

- **FUN3D and CFL3D results from 1409x641 grid**
- **Strand grid 40X coarser**

Dual Mesh Validation

Moving bodies

- **Added moving grid terms**

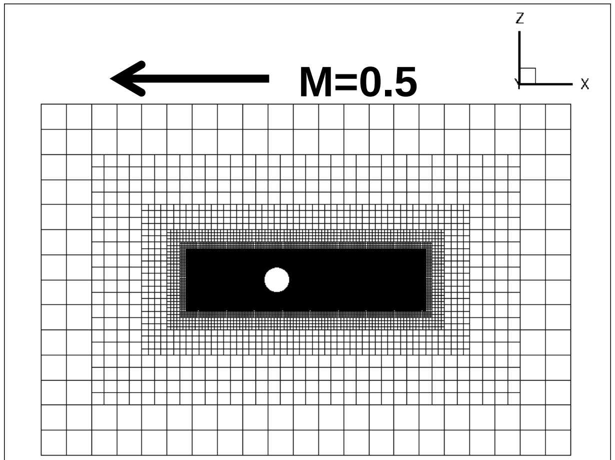

Moving sphere

	CD
Static	0.2861
*Moving	0.3002

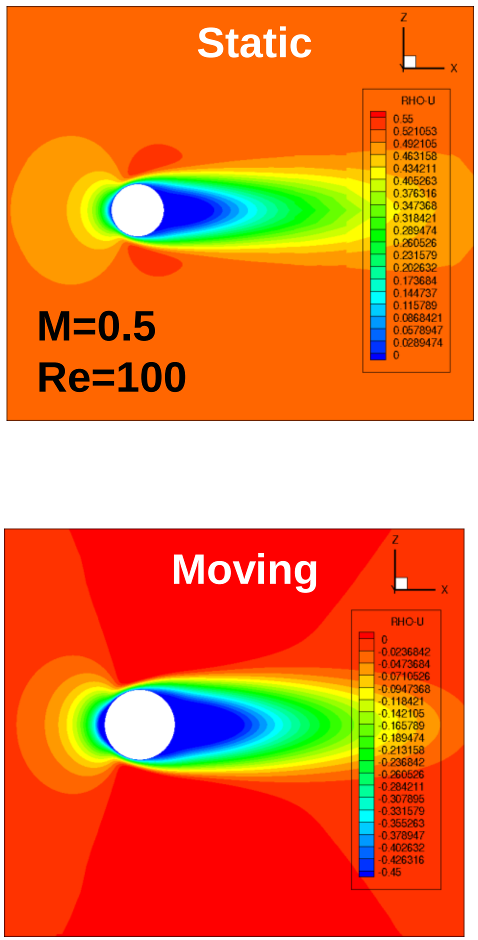

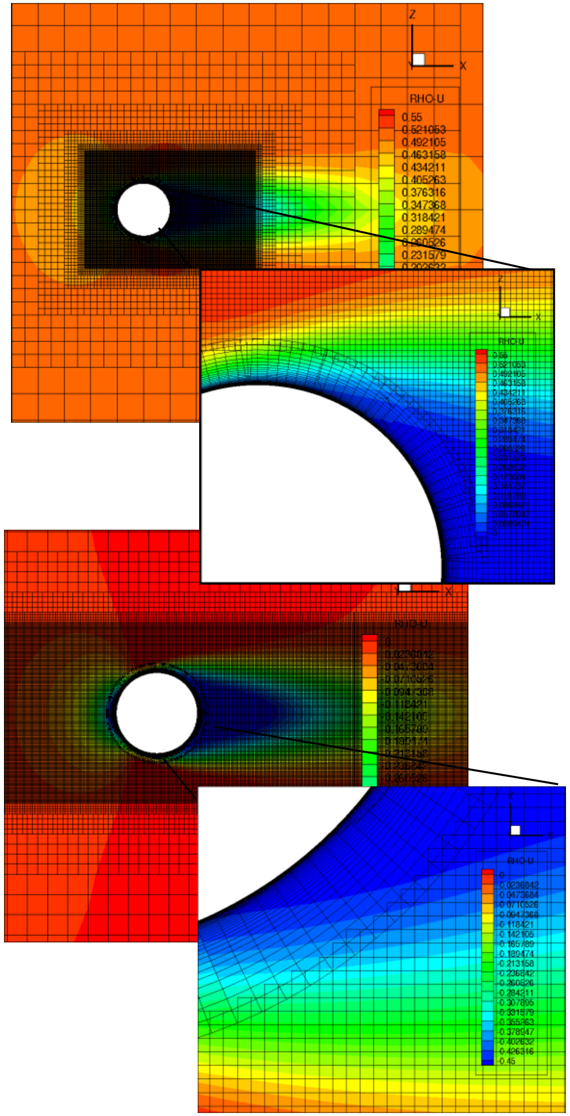

**Moving grid convergence limited by fine off-body grid extents*

Dual Mesh Validation

Timing comparison w Helios

- **Same mesh, Helios vs strand solver**
  - NSU3D run on strand mesh
  - strand solver cell-centered, more DOF

M=0.3
Re=100
10K steps
Steady

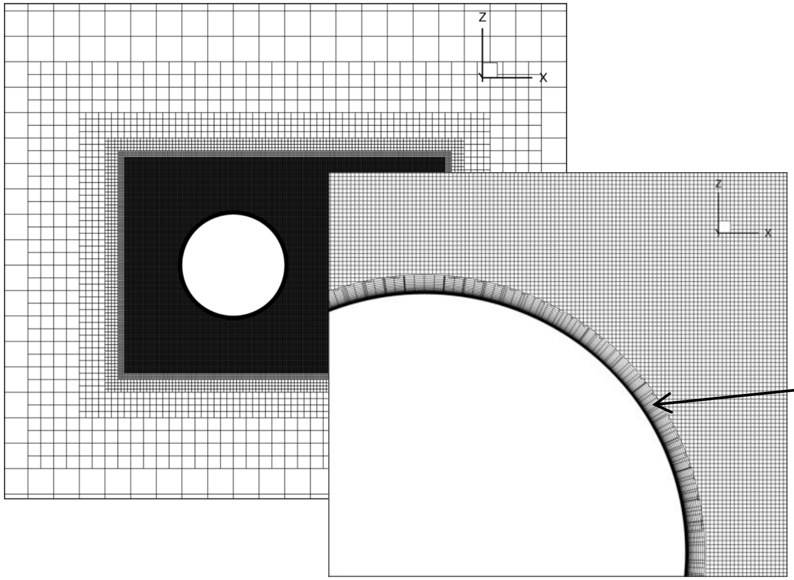

Diameter = 2.0
Strand len = 0.1

	Helios	Strand
*Near-body	0.086s	0.604s
Off-body	1.82s	1.75s
Domain connectivity	6.26e-3	7.42e-3

**Strand solver uses more DOF than Helios*

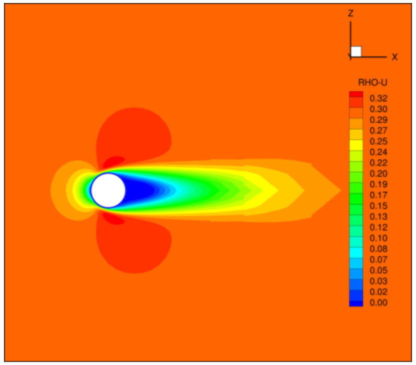

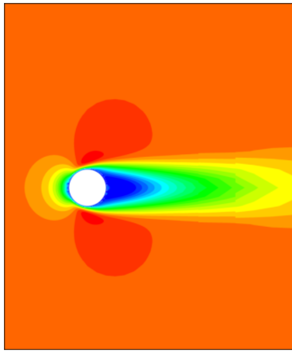

Dual Mesh Validation

Turbulent bluff body

- **Helios implementation**
  - Strand near-body
  - SAMARC off-body
- **Bluff body separated flow over sphere**
  - M = 0.3, Re = 12.0E6
  - Dual mesh
  - Adaptive

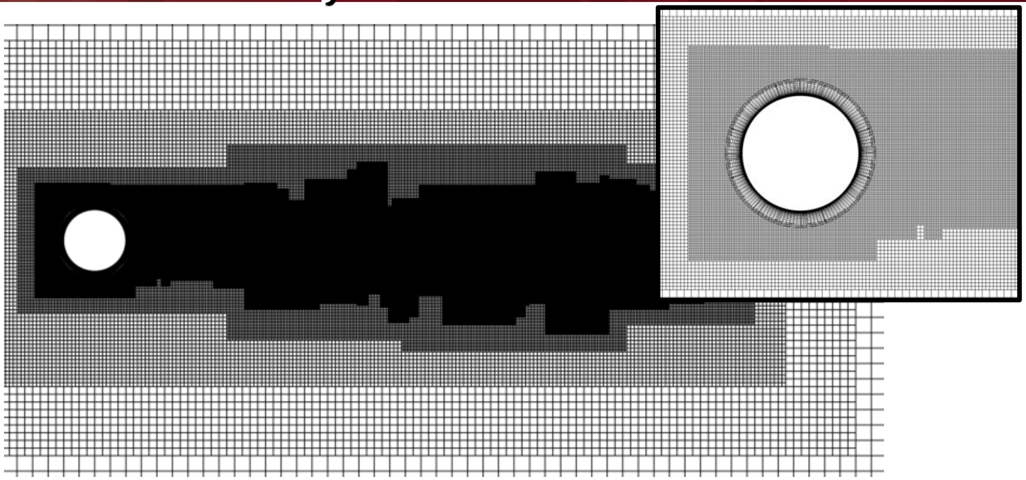

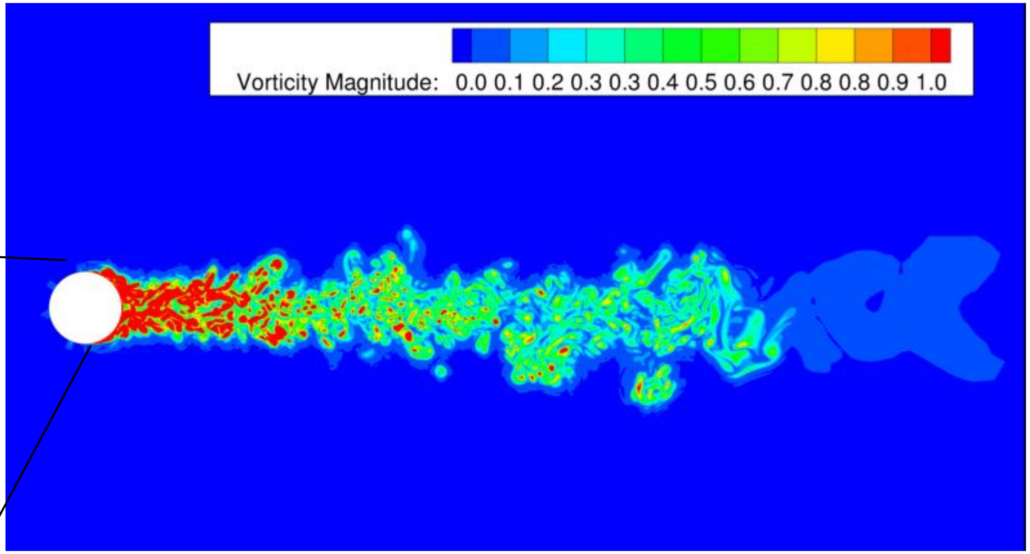

Vorticity

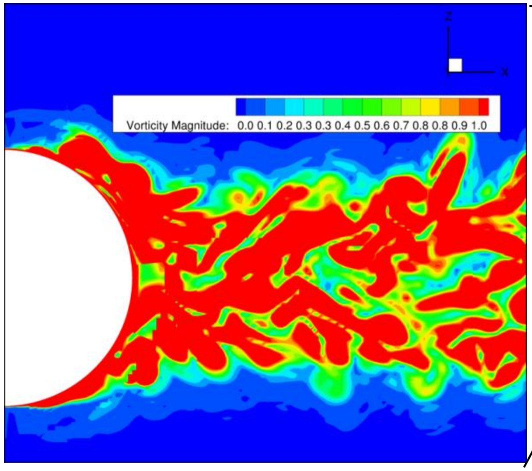

3D Wing

- **NACA 0015 Wing**
  - Aspect Ratio = 6.6
  - M = 0.1235, Re = 1.5E6
  - Dual mesh
  - Adaptive

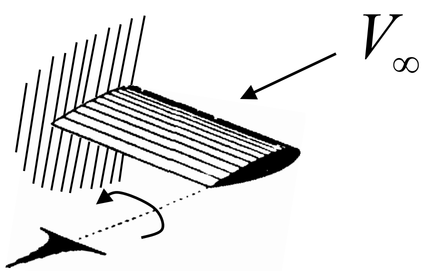

M_∞= 0.1235, α =12^o

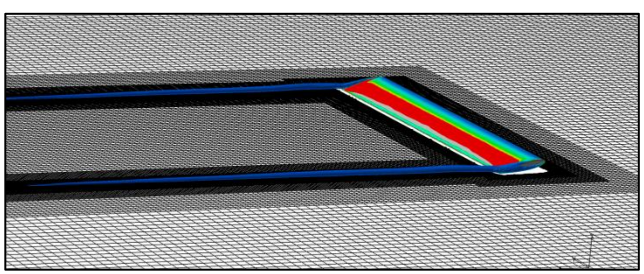

Strand

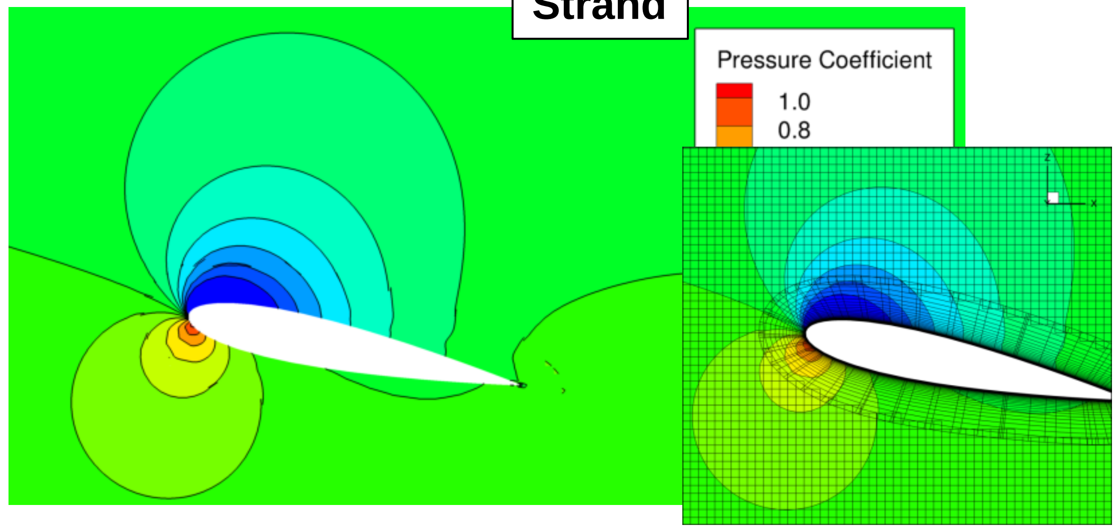

Helios v4

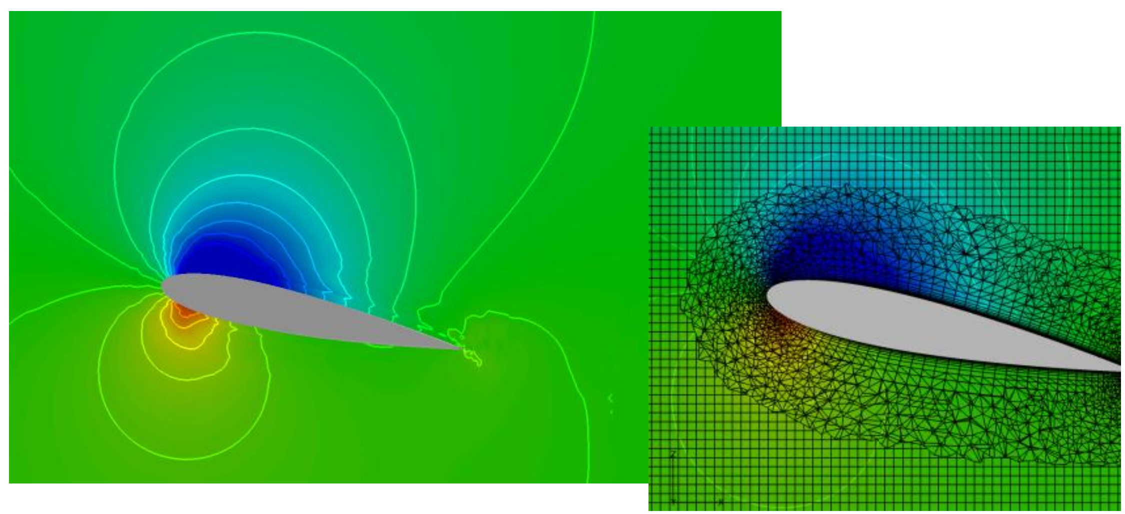

Computational Efficiency

- **4^{th} order strand-based FV scheme order of magnitude cheaper than Discontinuous Galerkin (DG) methods**
  – Standard finite differences in normal (strand) direction
  – Standard finite volume flux correction in streamwise directions

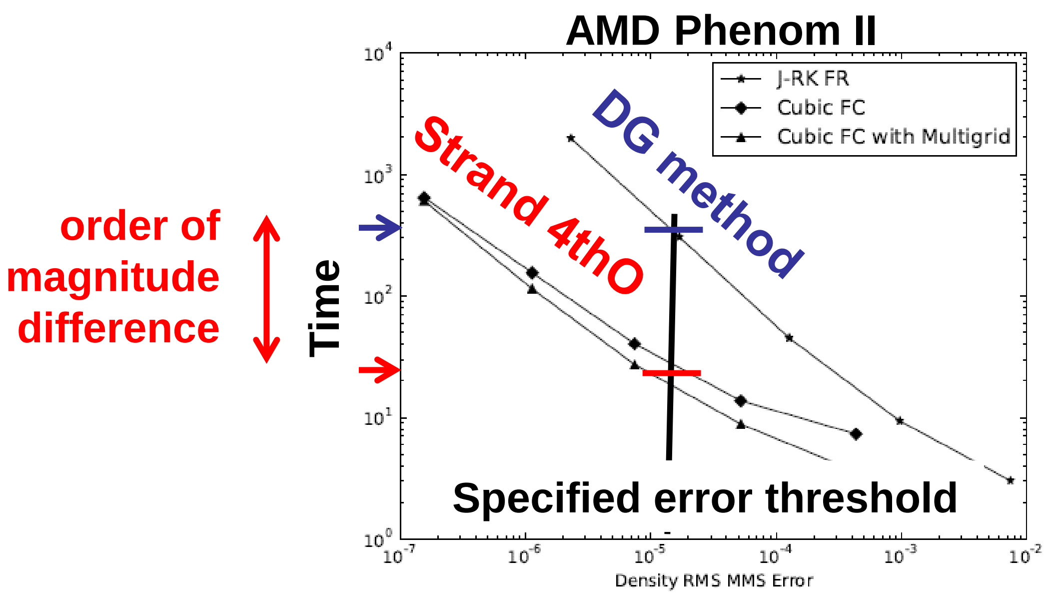

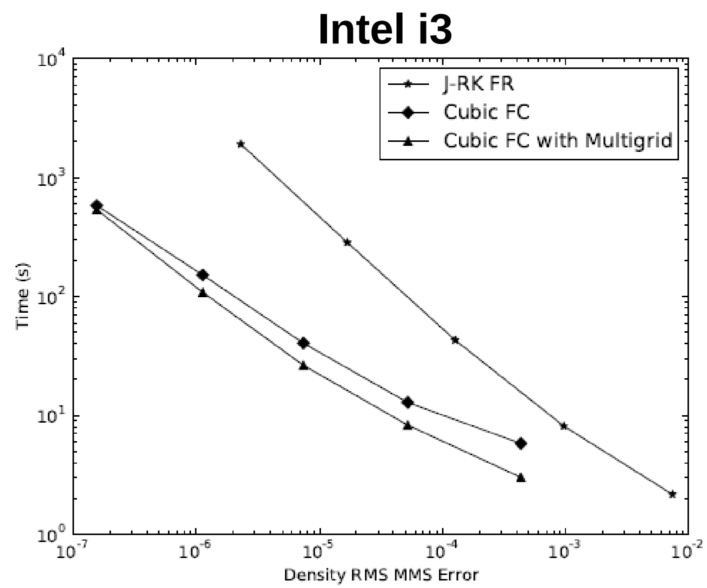

Courtesy D. Work, Utah St.

Cost of 4^{th} order scheme comparable to standard 2^{nd} order

Summary & Conclusions

- **Strand technology will improve automation, accuracy, and efficiency in Helios**
- **In past OGS meetings we have reported on strand-specific meshing infrastructure (PICASSO) and domain connectivity (OSCAR)**
- **Present development focus is an efficient high-order near-body strand solver**
  - Achieve up to 4th-order through a combination of finite difference and flux correction operations
  - Cost comparable to standard 2nd-order FV methods; order of magnitude cheaper than high order finite element (DG) methods
  - Accuracy on par with established FUN3D, CFL3D codes
- **Anticipate initial capability release in Helios v6 (Summer 2015)**
  - Multiple bodies
  - Complex geometries

Acknowledgements

Material presented is a product of the CREATE AV element of the Computational Research and Engineering for Acquisition Tools and Environments (CREATE) program sponsored by the U.S. Dept. of Defense HPC Modernization Program Office.

DISCLAIMER: **Reference herein to any specific commercial, private or public products, process, or service by trade name, trademark, manufacturer, or otherwise, does not constitute or imply its endorsement, recommendation, or favoring by the United States Government. The views and opinions expressed herein are strictly those of the authors and do not represent or reflect those of the United States Government. The viewing of the presentation by the Government shall not be used as a basis of advertising.**